

Chalcogen Extrusion from Heteroallenes and Carbon Monoxide by a Three-Coordinate Rh(I) Disilylamide

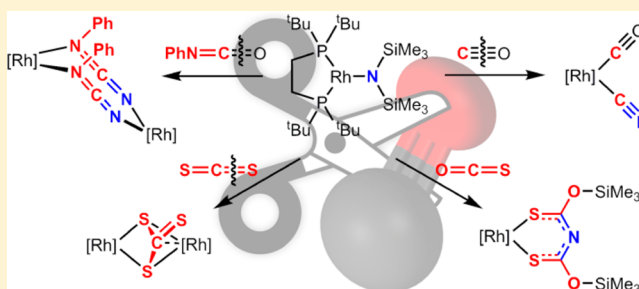
Matthew T. Whited,^{*,†} Lisa Qiu,[†] Alex J. Kosanovich,[†] and Daron E. Janzen[‡]

[†]Department of Chemistry, Carleton College, Northfield, Minnesota 55057, United States

[‡]Department of Chemistry and Biochemistry, St. Catherine University, St. Paul, Minnesota 55105, United States

S Supporting Information

ABSTRACT: We report the reactions of several heteroallenes (carbon disulfide, carbonyl sulfide, and phenyl isocyanate) and carbon monoxide with a three-coordinate, bis(phosphine)-supported Rh(I) disilylamide (**1**). Carbon disulfide reacts with **1** to afford a silyltrithiocarbonate complex similar to an intermediate previously invoked in the deoxygenation of CO₂ by **1**, and prolonged heating affords a structurally unusual μ - κ^2 (S,S'): κ^2 (S,S')-trithiocarbonate dimer. Carbonyl sulfide reacts with **1** to afford a structurally unique Rh(SCNCS) metallacycle derived from two insertions of OCS and N-to-O silyl-group migrations. Phenyl isocyanate reacts with **1** to afford a dimeric bis(phenylcyanamido)-bridged complex resulting from multiple silyl-group migrations and nitrogen-for-oxygen metathesis, akin to reactivity previously observed with carbon dioxide. The ability of **1** to activate carbon–chalcogen multiple bonds via silyl-group migration is further supported by its reactivity with carbon monoxide, where a nitrogen-for-oxygen metathesis is also observed with expulsion of hexamethyldisiloxane. For all reported reactions, intermediates are observable under appropriate conditions, allowing the formulation of mechanisms where insertion of the unsaturated substrate is followed by one or more silyl-group migrations to afford the observed products. This rich variety of reactivity confirms the ability of metal silylamides to activate exceptionally strong carbon–element multiple bonds and suggests that silylamides may be useful intermediates in nitrogen-atom and nitrene-group-transfer schemes.



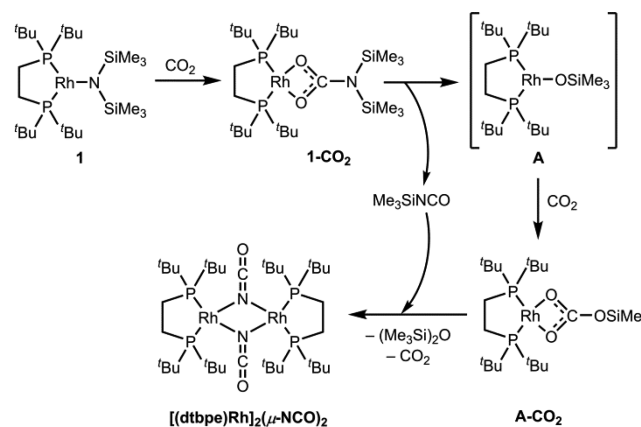
INTRODUCTION

Because of their utility in catalytic C–N bond-forming processes,¹ late-metal amides have been the subject of numerous synthetic, structural, and reactivity studies.² Silylamides have proven particularly useful for allowing access to novel late-metal amido structures because of their lower basicity and reducing power relative to alkyl-substituted amides.^{2a,b,3} Exploiting the stability of the M–N linkage in such complexes, Fryzuk and Caulton have utilized PNP pincer-type ligands containing a central disilylamide donor to support a range of structures and reactivity at late metals.⁴ Nevertheless, the N–Si bond in silylamido metal complexes is known to be both kinetically labile and thermodynamically unstable under a variety of conditions,⁵ particularly in instances where strong Si–O or Si–F bonds can be formed.

As part of a research program focused on developing metal/silicon cooperative approaches to small-molecule activation,⁶ we have recently begun investigating late-metal silylamides with an eye toward exploiting the instability of the N–Si bond to deliver nitrogen-based groups to a variety of substrates. We showed that a three-coordinate rhodium(I) disilylamide ((dtbpe)Rh–N(SiMe₃)₂, **1**) supported by the 1,2-bis(di-*tert*-butylphosphino)ethane (dtbpe) ligand reacts with carbon dioxide to afford a bis(μ -isocyanate) rhodium dimer, the product of a net nitrogen-for-oxygen metathesis.^{6b} The rate of

the reaction is slow enough to allow NMR observation of two intermediates, and a combination of spectroscopic and reactivity studies allowed formulation of a detailed mechanism for the transformation (Scheme 1). However, all attempts to

Scheme 1. Proposed Mechanism for CO₂ Deoxygenation by **1**



Received: February 7, 2015

Published: March 23, 2015

isolate and structurally characterize the carbamate (1-CO_2), monomeric trimethylsiloxide (**A**), and silylcarbonate (A-CO_2) intermediates proved unfruitful due to their instability under the reaction conditions.

Here we extend our earlier studies to a variety of heteroallene relatives of CO_2 , including carbon disulfide, carbonyl sulfide, and phenyl isocyanate, as well as carbon monoxide. The studies not only substantiate our earlier proposed reaction mechanism for CO_2 but also show that **1** participates in a rich array of reaction pathways with substrates containing carbon–chalcogen multiple bonds. In all cases, the reactions involve one or more insertions of the unsaturated substrate into the Rh–N bond followed by multiple silyl-group migrations. For CS_2 , PhNCO, and CO, the major product recovered results from one or more carbon–chalcogen bond cleavages, though the structures are quite distinct from one another. For carbonyl sulfide, the reaction affords a structurally unique $\text{Rh}(\text{SCNCS})$ six-membered metallacycle where the exocyclic C–O bonds remain intact.

RESULTS AND DISCUSSION

Reactivity of $(\text{dtbpe})\text{Rh-N}(\text{SiMe}_3)_2$ with Carbon Disulfide. We began our studies by seeking to extend the reactivity previously demonstrated with carbon dioxide to the most similar heteroallene, carbon disulfide. The reaction of **1** with CS_2 initially follows a similar course to the reaction of **1** with CO_2 . An immediate color change from dark green to dark red-brown is observed upon addition of CS_2 to a solution of **1**, along with formation of a new species observed by ^{31}P NMR (δ 111.3 (d, $^1J_{\text{RhP}} = 183$ Hz)). We assign this species as the rhodium dithiocarbamate 1-CS_2 derived from CS_2 insertion into the Rh–N bond of **1**, by analogy with previously reported CO_2 reactivity of **1**. The formation of 1-CS_2 is accompanied by a slight upfield shift (from 0.64 to 0.52 ppm) of the trimethylsilyl resonance by ^1H NMR spectroscopy, consistent with previous observations for the related carbamate complex 1-CO_2 .

Dithiocarbamate 1-CS_2 was unstable under these conditions, immediately beginning to decompose to a second species (**2**) with a very similar ^{31}P chemical shift (δ 110.7 (d, $^1J_{\text{RhP}} = 182$ Hz)) and a single trimethylsilyl group observed by ^1H NMR (δ 0.44). Over the course of 1 h, **3** was generated quantitatively along with **1** equiv of (trimethylsilyl)isothiocyanate, TMS-NCS (^1H NMR: δ –0.21). Spectroscopic similarities between **2** and 1-CS_2 suggested that **2** is a silyltrithiocarbonate complex, analogous to the silylcarbonate complex A-CO_2 formed as an intermediate in the reaction of **1** with CO_2 . Single crystals of **2** were grown from pentane/hexamethyldisiloxane (HMDSO), and X-ray crystallography confirmed that **2** is a silyltrithiocarbonate complex (Figure 1), with the rhodium center adopting an approximately square-planar geometry. Although silyl-substituted trithiocarbonate complexes have not been reported, alkyltrithiocarbonates (also known as thioxanthates) are well-known. Moreover, alkyltrithiocarbonates are generally prepared by CS_2 insertion into a metal thiolate,⁷ providing support for a mechanism where **2** is formed via an unobserved rhodium(I) silylthiolate intermediate (Scheme 2).

Though trithiocarbonate complex **2** could be crystallographically characterized, it was found to be unstable in solution for extended periods, decomposing quantitatively to a new $(\text{dtbpe})\text{Rh}$ product, **3** (^{31}P NMR: δ 106.7 ($^1J_{\text{RhP}} = 189$ Hz)), with concomitant formation of hexamethyldisilathiane, $(\text{Me}_3\text{Si})_2\text{S}$ (^1H NMR: δ 0.30; ^{13}C NMR: δ 4.2). Although this

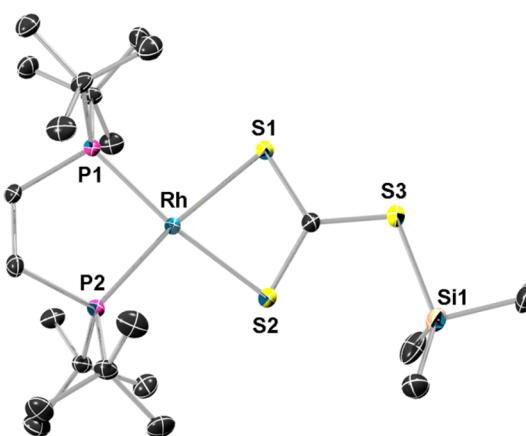
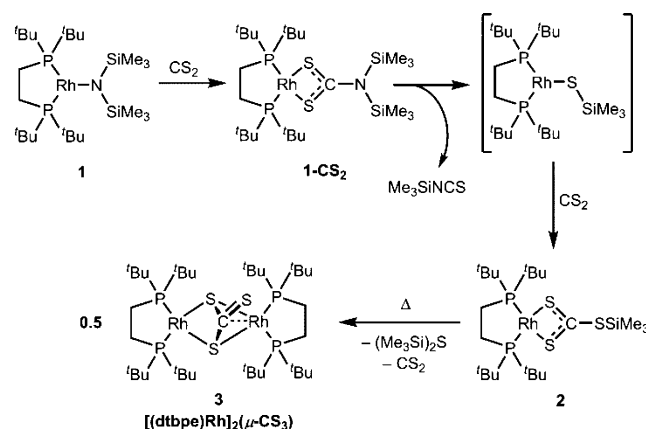


Figure 1. Solid-state structure of $(\text{dtbpe})\text{RhS}_2\text{CSSi}(\text{CH}_3)_3$ (**2**) with thermal ellipsoids at the 50% probability level and hydrogen atoms omitted for clarity. Selected bond lengths (Å) and angles (deg): Rh–P1, 2.235(2); Rh–P2, 2.242(2); Rh–S1, 2.393(2); Rh–S2, 2.394(2); S1–C19, 1.683(7); S2–C19, 1.695(7); S3–C19, 1.737(6); P1–Rh–P2, 87.73(6); P1–Rh–S1, 99.97(5); P1–Rh–S2, 172.20(6); P2–Rh–S1, 170.67(6); P2–Rh–S2, 99.69(6); S1–Rh–S2, 72.87(6).

Scheme 2. Proposed Mechanism of CS_2 Desulfurization by **1**



finding parallels previous studies where HMDSO was observed during conversion of the analogous silylcarbonate to a bis(μ -isocyanate) dimer, it was found that the conversion of **2** \rightarrow **3** occurred cleanly in the presence or absence of TMS-NCS , since a crystalline sample of **2** free of TMS-NCS could be cleanly and quantitatively converted to **3** by moderate heating (12 h, 80 $^\circ\text{C}$) in benzene. The identity of **3** was ultimately determined by X-ray crystallography, revealing a dimeric structure with a bridging trithiocarbonate ligand (Figure 2). Though the **2** \rightarrow **3** conversion must involve two molecules of **2**, it is not known whether CS_2 deinsertion from one molecule of **2** occurs before or after the bimolecular step where $(\text{Me}_3\text{Si})_2\text{S}$ is formed. Though a similar pathway could be envisioned for the analogous silylcarbonate complex A-CO_2 , it is unclear whether such a reaction is possible since A-CO_2 is unstable in the presence of TMS-NCO and cannot be isolated free of the silylisocyanate.

The bridging mode exhibited by CS_3^{2-} in **3** is unusual⁸ and, to the best of our knowledge, has not previously been crystallographically characterized. Bridging trithiocarbonate ligands normally adopt $\mu\text{-}\kappa^1(\text{S}):\kappa^2(\text{S}',\text{S}'')$ ⁹ or $\mu\text{-}\kappa^2(\text{S},\text{S}'):\kappa^2(\text{S}',\text{S}'')$ ¹⁰ binding modes (Figure 3), whereas in this case a $\mu\text{-}\kappa^2(\text{S},\text{S}'):\kappa^2(\text{S},\text{S}')$ mode is exhibited, where the same two sulfur

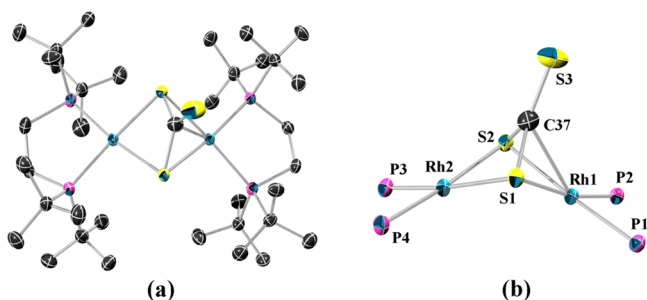


Figure 2. (a) Solid-state structure of $[(\text{dtbpe})\text{Rh}]_2(\mu\text{-CS}_3)$ (**3**) with thermal ellipsoids at the 50% probability level and hydrogen atoms and a cocrystallized molecule of diethyl ether omitted for clarity and (b) labeled solid-state structure of the core of **3**. Selected bond lengths (Å) and angles (deg): Rh1–P1, 2.2741(13); Rh1–P2, 2.2655(14); Rh1–S1, 2.3836(13); Rh1–S2, 2.3855(13); Rh1–C37, 2.311(6); Rh2–P3, 2.2546(14); Rh2–P4, 2.2509(15); Rh2–S1, 2.3715(13); Rh2–S2, 2.3660(14); C37–S1, 1.774(6); C37–S2, 1.775(5); C37–S3, 1.668(5); Rh1–S1–Rh2, 92.28(5); Rh1–S2–Rh2, 92.37(5).

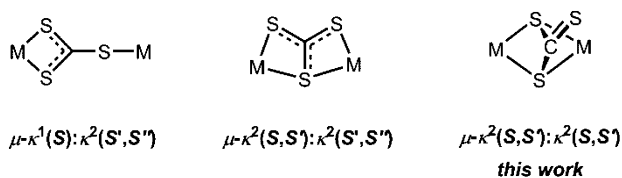


Figure 3. Binding modes of $\mu\text{-CS}_3^{2-}$.

atoms bind to each metal center. Each rhodium adopts an approximately square-planar configuration, and the structure is bent at the $\mu\text{-CS}_3$, creating an angle between S–Rh–S planes of 52.8° , nearly identical to what was previously observed by Jones for a related bis($\mu\text{-SH}$) dimer (54.5°).¹¹ There is an additional short contact (2.310(6) Å) in the solid state between carbon and one rhodium, but this interaction is clearly fluxional in solution, leading to apparent D_{2h} symmetry on the NMR time scale. The crystal structure most similar to **3** is from an S-alkylated derivative of a dimolybdenum $\mu\text{-CS}_3$ complex reported by DuBois and co-workers.¹² The methyltrithiocarbonate complex not only contains identically bridging sulfur atoms but also evinces one C–Mo interaction (2.20 Å) that is significantly shorter than that in the structure of **3**.

Reactivity of $(\text{dtbpe})\text{Rh-N}(\text{SiMe}_3)_2$ with Oxygen-Containing Heteroallenes: Carbonyl Sulfide and Phenyl Isocyanate. In light of the distinct reactivity with **1** observed for carbon disulfide versus carbon dioxide, we determined to examine carbonyl sulfide ($\text{O}=\text{C}=\text{S}$), which contains both sulfur and oxygen atoms as silyl-group acceptors. Addition of an excess of OCS (1 atm) to a solution of **1** in C_6D_6 led to an immediate color change from dark green to red, and ^{31}P NMR spectroscopy confirmed conversion to a single major (>90%) product **4** (δ 91.6 (d, $^1J_{\text{RhP}} = 160$ Hz)) with a concomitant upfield shift in the trimethylsilyl resonance (from 0.64 to 0.12 ppm). However, no TMS–NCO, TMS–NCS, HMDSO, or $(\text{Me}_3\text{Si})_2\text{S}$ was observed, indicating that the reaction follows a significantly different path from the reaction with CO_2 or CS_2 . When less OCS (0.4 atm) was utilized, the reaction proceeded slowly enough to allow observation of an intermediate species with inequivalent phosphines assigned as the product of a single OCS insertion into the Rh–N bond, **1-OCS** (^{31}P NMR: δ 108.6 (dd, $^1J_{\text{RhP}} = 189$ Hz, $^2J_{\text{PP}} = 27$ Hz), 125.6 (dd, $^1J_{\text{RhP}} = 206$ Hz, $^2J_{\text{PP}} = 27$ Hz); ^1H NMR (Me_3Si resonance only): δ 0.45),

though the reaction ultimately afforded numerous side products in addition to **4** under these conditions.

The identity of the complex **4** was finally determined by X-ray crystallography (Figure 4), revealing a structurally unique

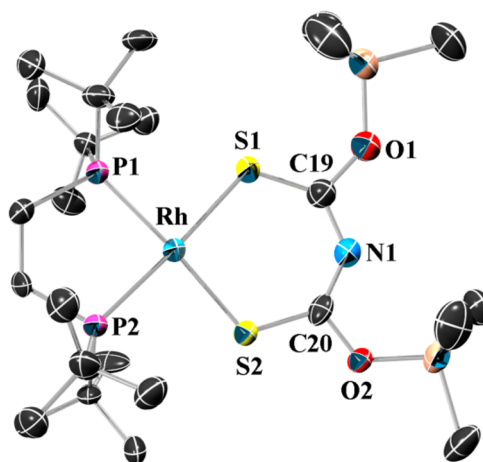
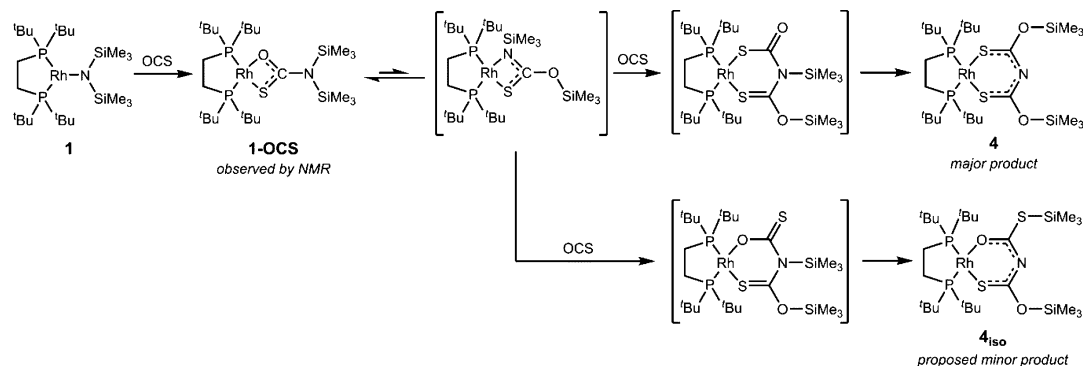


Figure 4. (a) Solid-state structure of $(\text{dtbpe})\text{Rh}(\text{SC}(\text{OSiMe}_3))_2\text{N}$ (**4**) with thermal ellipsoids at the 50% probability level and hydrogen atoms omitted for clarity. Selected bond lengths (Å) and angles (deg): Rh–P1, 2.315(3); Rh–P2, 2.310(3); Rh–S1, 2.307(3); Rh–S2, 2.307(3); P1–Rh–P2, 86.0(1); P1–Rh–S1, 90.7(1); P1–Rh–S2, 174.4(1); P2–Rh–S1, 173.9(1); P2–Rh–S2, 90.5(1); S1–Rh–S2, 93.1(1).

$\text{Rh}(\text{SCNCS})$ metallacycle derived from insertion of two molecules of carbonyl sulfide and two silyl-group migrations, one to each oxygen. Thus, in contrast to observations for all other substrates, the $\text{C}=\text{O}$ and $\text{C}=\text{S}$ bonds are not broken by reaction with **1**, only weakened by insertion and silyl-group migration. The $(\text{SCNCS})^-$ ligand is isoelectronic with the ubiquitous acetylacetonate (acac) ligands or bidentate malonate esters. Complex **4** exhibits an approximately square-planar geometry about the rhodium center, similar to crystallographically characterized bis(phosphine) rhodium acac complexes.¹³

A proposed mechanism for the **1** \rightarrow **4** conversion is presented in Scheme 3. Though the initial insertion product, **1-OCS**, can be observed under appropriate conditions, no other intermediates were identified for this reaction. On the basis of related results, we propose that **1-OCS** likely undergoes a silyl-group migration from nitrogen to oxygen and rearrangement prior to insertion of a second equivalent of OCS. However, our failure to observe the rearranged species suggests either that isomerization of **1-OCS** is slow relative to OCS insertion under the conditions examined or that it is reversible, with equilibrium favoring **1-OCS**. In either case, insertion of carbonyl sulfide appears to occur preferentially to the N,S-bound isomer rather than to the O,S-bound isomer.

Under the conditions examined, we also noted the formation of a minor product (ca. 2%) that could not be separated from **4** by crystallization. We propose that this product, denoted as **4_{iso}**, is likely an unsymmetrical isomer of **4** based on its inequivalent phosphine and trimethylsilyl environments observed by NMR spectroscopy as well as the fact that it did not noticeably affect combustion analysis results. Considering the proposed mechanism (Scheme 3), the formation of **4_{iso}** versus **4** would be determined by the regioselectivity of the second OCS insertion and subsequent silyl-group migration. Our finding of

Scheme 3. Proposed Mechanism for Reaction of **1** with OCS

preferential silyl-group migration to oxygen versus sulfur is consistent with previous studies showing that insertion reactions involving silylamines and carbonyl sulfide preferentially form O-silyl products.¹⁴

Recognizing that a nitrene substituent is isoelectronic with oxygen or sulfur, we sought to deepen our understanding of the interactions of **1** with oxygen-containing heteroallenes by examining the reaction of **1** with phenyl isocyanate. Upon addition of a small excess (2–4 equiv) of phenyl isocyanate to a solution of **1**, the slow insertion of phenyl isocyanate to give **1-PhNCO** was observed (³¹P NMR: δ 118.7 (dd, $^1J_{\text{RhP}} = 114$ Hz, $^2J_{\text{PP}} = 34$ Hz), 120.0 (dd, $^1J_{\text{RhP}} = 105$ Hz, $^2J_{\text{PP}} = 34$ Hz); ¹H NMR (Me₃Si resonance only): δ 0.27), consistent with our findings for other heteroallenes. As with the OCS reaction, the C_s-symmetric insertion product possesses inequivalent phosphine ligands. Complex **1-PhNCO** decays slowly (ca. 24 h) to afford a single major (>80%) rhodium product (**5**) with two inequivalent but uncoupled phosphine environments observed by ³¹P NMR (δ 100.7 (d, $^1J_{\text{RhP}} = 195$ Hz), 112.5 (d, $^1J_{\text{RhP}} = 194$ Hz)). During the reaction, any excess phenyl isocyanate is catalytically trimerized to phenyl isocyanurate (the trimer of phenyl isocyanate), as identified by crystallography¹⁵ and ¹H NMR and IR spectroscopies;¹⁶ when large excesses (>4 equiv) of PhNCO are utilized, phenyl isocyanurate is the major product of the reaction.

Complex **5** was identified by X-ray crystallography as a dirhodium species with the metals bridged by two phenylcyanamido ligands to give inequivalent rhodium centers (Figure 5). Bridging phenylcyanamide ligands are known,¹⁷ and cyanamides have been used as linkers for preparing multimetallic complexes.¹⁸ The crystallographically characterized compound most similar to **5** is a dimer with two phenylcyanamido ligands bridging bis(triphenylphosphine)-supported copper(I) centers,^{17a} with the distinction that cyanamide ligands in **5** bridge unsymmetrically, creating two distinct rhodium(I) environments. IR spectroscopy provides additional support for the presence of phenylcyanamide ligands, with an intense absorbance at 2157 cm⁻¹.¹⁹ On the basis of the unsymmetrical phenylcyanamide bridging mode, **5** may be viewed as a zwitterion with positive and negative charges localized at the distinct Rh(I) centers. However, resonance through the phenylcyanamide ligands likely negates any significant charge separation, consistent with the solubility of **5** in nonpolar solvents such as pentane.

Though cyanamide ligands are relatively common, they are typically generated by deprotonation of cyanamide derivatives^{17b} or reaction of a metal nitride with an isocyanide.²⁰ The net process reported herein provides a potentially distinct route

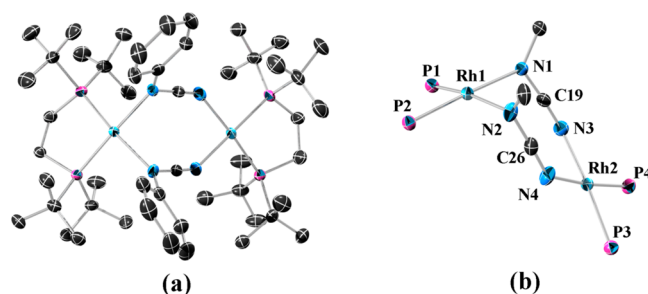
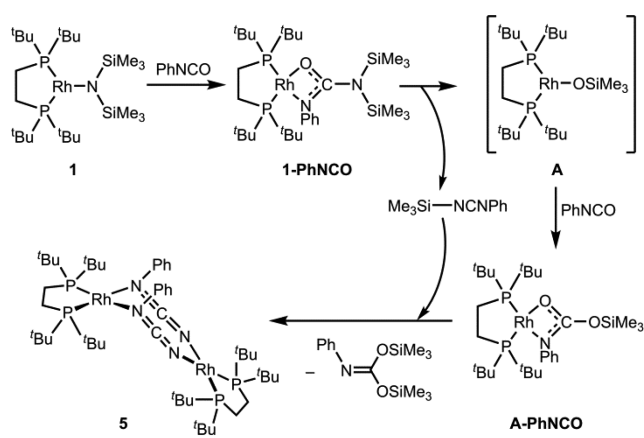


Figure 5. (a) Solid-state structure of $[(\text{dtbpe})\text{Rh}]_2(\mu\text{-PhNCN})_2$ (**5**) with thermal ellipsoids at the 50% probability level and hydrogen atoms omitted for clarity and (b) labeled solid-state structure of the core of **5**. Selected bond lengths (Å) and angles (deg): Rh1–P1, 2.2385(11); Rh1–P2, 2.2486(12); Rh1–N1, 2.186(4); Rh1–N2, 2.183(4); N1–C19, 1.304(5); C19–N3, 1.164(5); N2–C26, 1.295(5); C26–N4, 1.164(5); Rh2–P3, 2.2066(11); Rh2–P4, 2.2080(13); Rh2–N3, 2.112(4); Rh2–N4, 2.101(3); Rh1–N1–C19, 110.1(3); Rh1–N2–C26, 105.2(3); Rh2–N3–C19, 138.2(3); Rh2–N4–C26, 137.8(3).

to bridging cyanamide ligands from isocyanates, using silylamides as an N atom source. Related reactions have been reported for main-group silylamides, where reaction with isocyanates affords carbodiimides via isocyanate insertion and N-to-O silyl-group migration.²¹

Though the reaction of **1** with PhNCO does not proceed as cleanly as the reactions with other heteroallenes, we are able to postulate a likely mechanism based on several key observations:

1. 2 equiv of PhNCO are required for complete reaction. When only 1 equiv is utilized, the reaction stalls with an approximately 1:1 mixture of **1** and **5**.
2. As **1-PhNCO** disappears, another major (dtbpe)Rh species is formed and consumed during the **1** → **5** conversion. This species exhibits similar ³¹P NMR chemical shifts to those of **1-PhNCO** and, like **1-PhNCO**, has inequivalent, coupled phosphine environments (δ 120.8 (dd, $^1J_{\text{RhP}} = 153$ Hz, $^2J_{\text{PP}} = 34$ Hz), 122.0 (dd, $^1J_{\text{RhP}} = 169$ Hz, $^2J_{\text{PP}} = 34$ Hz); ¹H NMR (Me₃Si resonance only): δ 0.26). By analogy with our other reactivity and spectroscopic similarities with A-CO₂ (vide supra),^{6b} we assign this intermediate as **A-PhNCO**, the product of phenyl isocyanate insertion into an unobserved rhodium trimethylsiloxy species **A** (Scheme 4).
3. Concomitant with the appearance of **A-PhNCO**, *N*-phenyl-*N'*-trimethylsilylcarbodiimide (TMS–NCNPh) is formed (¹H NMR (Me₃Si resonance only): δ 0.02).²² As

Scheme 4. Proposed Mechanism for Reaction of **1** with Phenyl Isocyanate

the reaction progresses and **5** is formed, the carbodiimide is consumed.

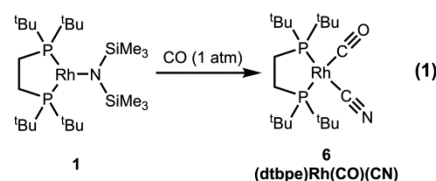
- In contrast to the previously reported reaction of **1** with CO_2 , HMDSO is not formed in significant quantities during the reaction of **1** with PhNCO. Instead, the major organic byproduct of the reaction of **1** with PhNCO (2 equiv) is assigned as bis(trimethylsilyl) *N*-phenylimidocarbonate ($\text{PhN}=\text{C}(\text{OSiMe}_3)_2$, Scheme 4) based on ^1H NMR spectroscopy (broad singlets at δ 0.26 and 0.21 representing distinct trimethylsilyl environments in a 1:1 ratio) and gas chromatography–mass spectrometry (GC-MS) analysis ($m/z = 281.1$) as well as the requirement for 2 equiv of PhNCO for complete conversion of **1**.

On the basis of the observations presented above, we propose that the formation of **5** from **1** and PhNCO follows a pathway similar to that observed for the reaction with CO_2 ^{6b} except for the final silyl-group transfer, which occurs from $\text{TMS}-\text{NCNPh}$ to the inserted intermediate **A-PhNCO** to release the imidocarbonate byproduct and (dtbpe)Rh-(NCNPh), which subsequently dimerizes to form **5** (Scheme 4). This mechanism would be completely analogous to Parkin's deoxygenation of CO_2 by a zinc bis(trimethylsilyl)amide complex, which gives a zinc isocyanate and bis(trimethylsilyl)-carbonate.^{5h} At this point, a bimetallic reaction pathway cannot be completely ruled out, though the proposed mechanism in Scheme 4 is most consistent both with the evidence in hand and other similar reactions reported herein.

Additional uncertainty surrounds the identity of the catalyst for isocyanate trimerization. It is possible that **1** or the initial insertion product **1-PhNCO** serves as the catalyst for isocyanurate formation, and indeed several metal amides have been shown to be active catalysts for the reaction.²³ However, the fact that isocyanurate is observed in significant quantities only in reactions with a large excess of PhNCO, where **1** is quickly consumed by PhNCO insertion, suggests that **1** is not the active catalyst. We also tested a pure sample of **5** and showed that it is not an active catalyst for PhNCO trimerization. Thus, it seems most likely that an as-yet unidentified side product formed during the **1** \rightarrow **5** conversion is responsible for isocyanurate formation.

Deoxygenation of Carbon Monoxide by (dtbpe)Rh-N(SiMe₃)₂. Having shown that the strong $\text{C}=\text{O}$ and $\text{C}=\text{S}$ bonds in carbon dioxide and carbon disulfide could be cleaved

by silyl migration with complex **1**, we were interested in whether the $\text{C}\equiv\text{O}$ bond of carbon monoxide could be similarly broken. The $\text{C}\equiv\text{O}$ bond in carbon monoxide is one of the strongest routinely encountered (257 kcal/mol, compared with 191 kcal/mol for $\text{C}=\text{O}$ in CO_2)²⁴ and is significantly stronger than $\text{C}\equiv\text{N}$ (213 kcal/mol) or $\text{N}\equiv\text{N}$ (226 kcal/mol). Thus, we were pleased to find that complex **1** reacts cleanly with CO to generate HMDSO and the C_s -symmetric product (dtbpe)-Rh(CO)(CN) (**6**, eq 1), where the carbon atom of the cyanide ligand is derived from CO. Complex **6** exhibits distinct phosphine environments, as evidenced by doublets of doublets in its ^{31}P NMR spectrum (δ 93.0 (dd, $^1J_{\text{RhP}} = 125$ Hz, $^2J_{\text{PP}} = 20$ Hz), 106.5 (dd, $^1J_{\text{RhP}} = 122$ Hz, $^2J_{\text{PP}} = 20$ Hz)). IR spectroscopic analysis of **6** shows intense diagnostic infrared bands for the cyanide and carbonyl ligands ($\nu_{\text{CN}} = 2104$ cm^{-1} , $\nu_{\text{CO}} = 1998$ cm^{-1}). Eisenberg reported a closely related complex, (dppe)Ir(CO)(CN), which exhibits similar ^{31}P NMR signals (without P/Rh coupling) and infrared signatures ($\nu_{\text{CN}} = 2119$ cm^{-1} , $\nu_{\text{CO}} = 1997$ cm^{-1}).²⁵



Deoxygenation of CO by silylamides is rare but has been observed. Sellmann reported that an unstable Ni(II) disilylamide reacts with carbon monoxide at low temperature to afford the corresponding Ni(II) cyanide complex without observable intermediates.²⁶ Parkin also described the reaction of lithium trimethylsilyl(alkyl)amides with a variety of metal carbonyl complexes, affording the corresponding isocyanides with loss of lithium trimethylsiloxide.²⁷ Parkin's transformations also proceeded without any reported intermediates, though the mechanism probably involves direct nucleophilic attack of amide on the bound carbonyl to form a carbamoyl intermediate that loses siloxide upon silyl-group migration. Finally, Wannagat and Seyffert showed some time ago that sodium bis(trimethylsilylamide) reacts directly with CO to give sodium cyanide and HMDSO, though the low electrophilicity of free CO means that the reaction only occurs under forcing conditions ($P_{\text{CO}} = 100$ atm), and the exact mechanism is unclear.²⁸

Our experiments provide a unique opportunity to formulate a mechanism for CO deoxygenation, since a long-lived intermediate can be observed during reaction. Exposure of a benzene solution of disilylamide **1** to CO (1 atm) leads to an immediate color change from dark green to yellow, along with the disappearance of the ^{31}P NMR signal corresponding to **1** and appearance of two new doublets of doublets (δ 70.7 ($^1J_{\text{RhP}} = 123$ Hz, $^2J_{\text{PP}} = 22$ Hz), 103.1 ($^1J_{\text{RhP}} = 137$ Hz, $^2J_{\text{PP}} = 22$ Hz)), indicating a species **1-CO** with two distinct phosphine environments. Over a period of ca. 2 h, intermediate **1-CO** converts to **6** (Figure 6). Although **6** also exhibits distinct phosphine environments, the ^{31}P chemical shifts and one-bond couplings to rhodium are much more similar to each other in **6** than in **1-CO**, suggesting that the phosphine environments in **1-CO** are quite distinct.

The reaction was observed to stall during conversion of **1-CO** \rightarrow **6** if less than 2 equiv of CO was utilized. However, addition of more CO led to fast and quantitative conversion of remaining **1-CO**. This finding suggests a mechanism where **1-**

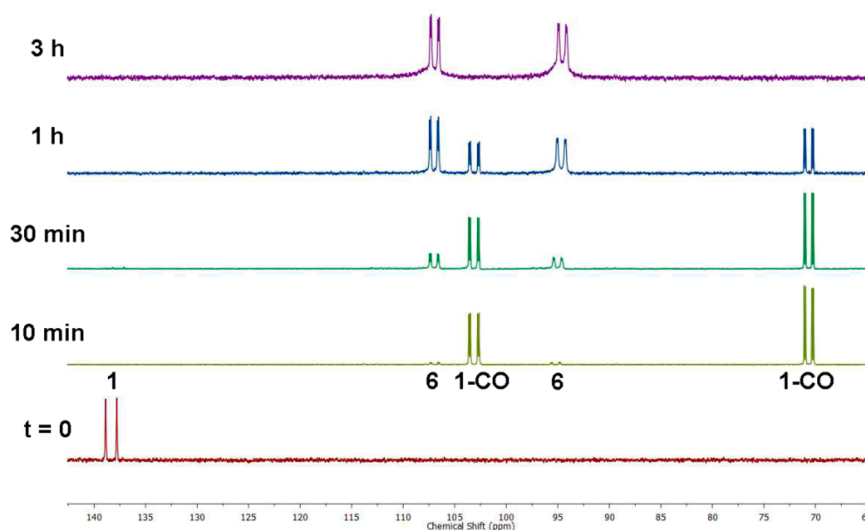


Figure 6. ^{31}P NMR spectra from reaction of **1** with CO (1 atm).

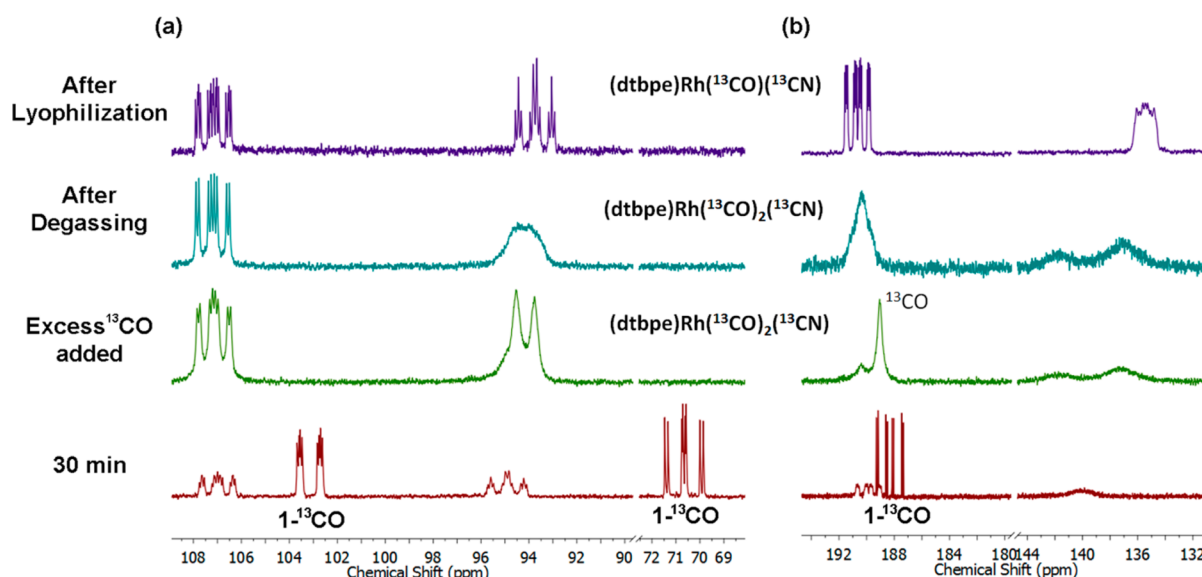


Figure 7. (a) ^{31}P NMR spectra from reaction of **1** with ^{13}CO ; (b) corresponding ^{13}C NMR spectra.

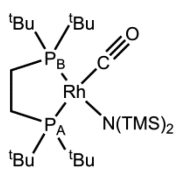
CO incorporates only 1 equiv of CO and an additional equivalent of CO is required to convert intermediate **1-CO** to **6**. Thus, we investigated the reaction of **1** with ^{13}CO to elucidate the nature of **1-CO** and confirm the structure of **6**. Upon exposure of an NMR sample of **1** in C_6D_6 to ^{13}CO (ca. 0.3 atm), an immediate color change from dark green to yellow was observed as $1\text{-}^{13}\text{CO}$ formed. ^{31}P NMR spectroscopy showed the same characteristic peaks as in Figure 6, but they were now split into doublets of doublets of doublets (ddd) because of two-bond coupling to ^{13}CO (Figure 7). As before, $1\text{-}^{13}\text{CO}$ slowly converted to $6(^{13}\text{C})$, though the low concentration of ^{13}CO in this case allowed us to stop the reaction at ca. 40% conversion after 30 min and fully characterize a mixture of $1\text{-}^{13}\text{CO}$ and $6(^{13}\text{C})$ by ^{13}C NMR spectroscopy (Figure 7, bottom).

As shown in Figure 7, $1\text{-}^{13}\text{CO}$ exhibits distinct ^{31}P environments with phosphines coupled to Rh, ^{13}C , and each other. The ^{13}C NMR spectrum of $1\text{-}^{13}\text{CO}$ shows a rhodium-bound carbonyl split by inequivalent phosphines and Rh into a ddd (Figure 7). The fact that there is a single CO ligand

associated with rhodium in a C_s -symmetric, square-planar environment supports the assignment of **1-CO** as the square-planar CO adduct of **1**, an assignment that is consistent with the substantially different phosphine environments (one trans to the amide, the other trans to a carbonyl) as well as observed coupling constants (Table 1).

Addition of excess ^{13}CO to a mixture of $1\text{-}^{13}\text{CO}$ and $6(^{13}\text{C})$ led to fast and complete formation of a complex with spectroscopic signatures similar to $6(^{13}\text{C})$ but with broadened and slightly shifted ^{31}P and ^{13}C signals for which not all coupling constants could be derived (Figure 7). Furthermore, the Rh- ^{13}CO peak in the ^{13}C NMR spectrum appeared to be in fast exchange with free ^{13}CO , with their broadened peaks nearly coalescing. Degassing the resulting mixture by three freeze-pump-thaw cycles allowed removal of ^{13}CO but did not sharpen the observed spectra. However, lyophilization of the product followed by redissolution in C_6D_6 restored the sharp spectral features expected for $(\text{dtbpe})\text{Rh}(^{13}\text{CO})(^{13}\text{CN})$ ($6(^{13}\text{C})$) (Figure 7, top). In light of Eisenberg's report that $(\text{dppe})\text{Ir}(\text{CO})(\text{CN})$ can reversibly bind CO to form $(\text{dppe})\text{-}$

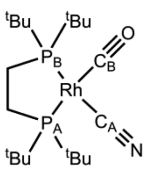
Table 1. Coupling Constants (in Hz) for 1-CO Observed by NMR Spectroscopy



nucleus	C	P _B	P _A
Rh	70	137	123
P _A	115	22	*
P _B	13	*	

$\text{Ir}(\text{CO})_2(\text{CN})$,²⁵ we conclude that **6** also reversibly binds an additional equivalent of carbon monoxide to form $(\text{dtbpe})\text{Rh}(\text{CO})_2(\text{CN})$ (**6-CO**).

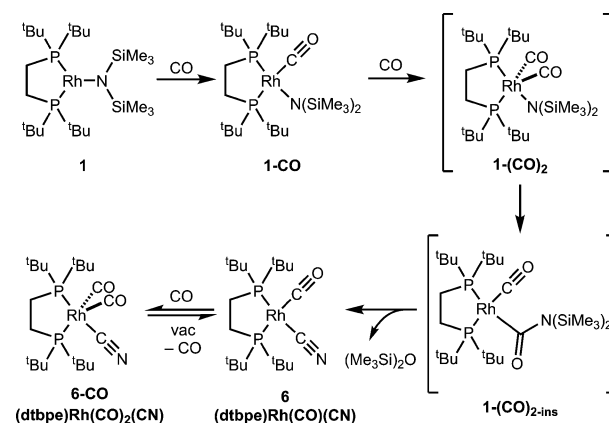
NMR and IR spectroscopy of **6** (¹³C) provide additional strong support for the formulation of **6** as $(\text{dtbpe})\text{Rh}(\text{CO})(\text{CN})$. Infrared spectroscopy of **6** (¹³C) shows intense infrared stretches associated with ¹³C≡N at 2059 cm⁻¹ ($\nu_{13\text{CN}} = 2060$ cm⁻¹, predicted) and ¹³C≡O at 1952 cm⁻¹ ($\nu_{13\text{CO}} = 1954$ cm⁻¹, predicted) at appropriately shifted values based on the harmonic oscillator approximation. Furthermore, the one- and two-bond coupling constants between ¹⁰³Rh, ³¹P, and ¹³C nuclei (Table 2) are consistent with a square-planar $(\text{dtbpe})\text{Rh}$ complex containing cis-disposed carbonyl and cyanide ligands.

Table 2. Coupling Constants (in Hz) for **6** Observed by NMR Spectroscopy


nucleus	C _B	C _A	P _B	P _A
Rh	^a	137	123	121
P _A	100	19	20	*
P _B	13	83	*	
C _A	7	*		

^aBroadening of the ¹³C signal by the attached ¹⁴N nucleus precluded accurate assignment of ¹J_{RhC} for the cyanide ligand.

Taken together, the experiments above support a mechanism (Scheme 5) for CO deoxygenation where **1** quickly binds a molecule of CO to afford the square-planar C_s-symmetric amido complex $(\text{dtbpe})\text{Rh}(\text{CO})(\text{N}(\text{SiMe}_3)_2)$ (**1-CO**). Insertion of CO into the Rh–N bond of **1-CO** could occur before or after coordination of an additional molecule of CO. By analogy with Landis's mechanism for hydroformylation by bis-(phosphine)rhodium complexes,³⁵ we currently favor a mechanism where CO coordinates to **1-CO** prior to migratory insertion. The resulting carbamoyl complex **1-(CO)₂** then undergoes facile conversion to **6** by a series of nitrogen-to-oxygen silyl-group migrations with release of HMDSO.

Scheme 5. Proposed Mechanism of CO Deoxygenation by Disilylamide **1**

CONCLUSIONS

In summary, we have reported a detailed synthetic study of the reactivity of a bis(phosphine)-supported rhodium disilylamide (**1**) with several heteroallenes and carbon monoxide. Disilylamide **1** affords a rich variety of reactivity with unsaturated, chalcogen-containing substrates, frequently giving products resulting from carbon–chalcogen multiple-bond cleavage and featuring unusual and in some cases unique structural motifs. For each substrate, we have provided evidence for a mechanism where insertion of the unsaturated molecule into a Rh–N bond activates it toward silyl-group migration to weaken and break carbon–element multiple bonds. This class of reactions promoted by **1** appears to be somewhat limited by the ability of the reacting partner to undergo insertion into the Rh–N bond. The importance of the insertion event is supported by our observation that nitrous oxide, which is isoelectronic with the heteroallenes examined, does not react with **1**, even at elevated temperatures. The lack of reactivity with N₂O stands in contrast to Sellmann's report for a Ni(II) bis(trimethylsilyl)amide complex, which in other respects exhibits reactivity similar to **1**.²⁶ However, comparisons are not easy to draw since the mechanisms by which Sellmann's system reacts are not well-understood due to the instability of the amide starting material and the fact that it undergoes reaction in minutes even at –78 °C.

This report has clearly demonstrated that, consistent with other findings, silylamides may serve as reactive nitrene-group and nitrogen-atom sources for substrates with suitable silyl-group acceptors, even activating the exceptionally strong C≡O bond of carbon monoxide. The work provides an interesting contrast with a report from Chirik on the reactivity of a μ -nitrido dihafnium isocyanate complex,²⁹ which also forms a cyanide ligand from CO by nitrogen/oxygen exchange, generating a μ -oxo dihafnium product. Whereas the hafnium reaction is a metal-based process relying on an oxophilic early metal to break the C≡O bond, the related reactions reported here utilize largely ligand-based processes to break carbon–oxygen and carbon–sulfur multiple bonds with formation of strong silicon–chalcogen bonds. The collective findings suggest that silylamides may be useful for a wide variety of transformations where silicon acts as a chalcogen or halogen acceptor and new nitrogen–carbon bonds are formed. Further studies in our laboratory will be directed both at expanding substrate scope for the unusual transformations of neutral

silylamides as well as targeting cationic late-metal silylamides as even more potent nitrene sources via R_3Si^+ removal.

EXPERIMENTAL SECTION

General Considerations. All manipulations were performed under a dinitrogen atmosphere in an MBraun Unilab 2000 glovebox or under an argon atmosphere using standard Schlenk techniques. Routine solvents were purchased from Aldrich and were deoxygenated and dried using a Glass Contour Solvent Purification System, except for anhydrous benzene and pentane, which were used as received from Aldrich. Chlorobis(cyclooctene)rhodium(I) dimer and silver(I) triflate were used as received from Strem. Lithium bis(trimethylsilyl)amide, carbon disulfide, carbonyl sulfide, phenyl isocyanate, and carbon monoxide (both unlabeled and ^{13}C -labeled) were used as received from Aldrich. The $(dtbpe)Rh(OTf)$ was prepared according to our previous report.^{6b,30} NMR solvents (Cambridge Isotope Laboratories) were degassed, passed through a pad of activated alumina, and stored over activated 3-Å molecular sieves prior to use. Alumina was activated by heating at 250 °C for 4 h under vacuum prior to use. NMR spectra were recorded at ambient temperature on a Varian Unity Plus 400 MHz spectrometer or Bruker Avance III HD 400 MHz spectrometer. 1H and ^{13}C NMR chemical shifts were referenced to residual solvent, and ^{31}P NMR chemical shifts are reported relative to an external standard of 85% H_3PO_4 . Infrared spectra were obtained on a Matteson Model 4020 Galaxy Series FTIR Spectrometer, and mass spectra were obtained on a Shimadzu QP-5000 GC/MS. Microanalysis was performed by Midwest Microlab, LLC.

$(dtbpe)Rh-N(SiMe_3)_2$ (1). This complex has been previously prepared and characterized.^{6b} For these studies, the instability of **1** rendered it most convenient to prepare and use immediately, so the following modified method was employed: To a chilled (−35 °C) solution of $(dtbpe)Rh(OTf)$ (40.7 mg, 0.0713 mmol) in diethyl ether (5 mL) was added lithium bis(trimethylsilyl)amide (0.0708 M solution in Et_2O , 1.01 mL, 0.0715 mmol) with stirring. Over a period of ca. 10 min, the solution changed color from red to deep green, and after 30 min the clean conversion of $(dtbpe)Rh(OTf)$ to **1** was confirmed by ^{31}P NMR spectroscopy (δ 137.8, $^1J_{RhP}$ = 175 Hz). Solvent was removed in vacuo to give a dark solid that was extracted into pentane (5 mL), filtered through a plug of Celite, and dried in vacuo to afford dark green crystals of **1** (36.7 mg, 88%) that were used without further purification.

$(dtbpe)RhS_2CSSi(CH_3)_3$ (2). Complex **1** (36.7 mg, 0.0631 mmol) was dissolved in C_6D_6 (700 μL), and carbon disulfide (two drops, ca. 20 μL) was added, causing the solution immediately to begin turning brown. The mixture was transferred to an NMR tube for monitoring (for details, vide supra). After 1 h, the reaction mixture consisted of ca. 90% of **2** by ^{31}P NMR; the mixture was transferred to a scintillation vial, and the volatiles were removed in vacuo to give a green-brown solid. The solid residue was dissolved in minimal pentane (ca. 1 mL), filtered, and set to crystallize by cross diffusion with HMDSO at −35 °C, affording a crop of dark green crystals suitable for X-ray diffraction after 24 h (14.1 mg, 37%). Because of the instability of **2** with respect to bimolecular decomposition to **3**, even freshly prepared NMR samples from crystalline **2** showed traces of **3** (ca. 10%). 1H NMR (400 MHz, C_6D_6): δ 0.43 (s, 9H, $SSi(CH_3)_3$), 1.19 (d, J = 12.6 Hz, 4H, $P(CH_2)_2P$), 1.24 (d, J = 11.9 Hz, 36H, $-C(CH_3)_3$). $^{13}C\{^1H\}$ NMR (101 MHz, C_6D_6): δ 1.3 ($SSi(CH_3)_3$), 23.7 (td, J_1 = 17 Hz, J_2 = 4 Hz, CH_2P), 30.9 (s, $C(CH_3)_3$), 37.2 (t, J = 8 Hz, $C(CH_3)_3$), 244.9 (s, RhS_2CS). $^{31}P\{^1H\}$ NMR (162 MHz, C_6D_6): δ 109.9 (d, $^1J_{RhP}$ = 183 Hz).

$[(dtbpe)Rh]_2(\mu-\kappa^2(S,S')\kappa^2(S',S')-CS_3)$ (3). Crystalline complex **2** (14.1 mg, 0.0234 mmol) was dissolved in C_6D_6 (700 μL) and heated at 80 °C for 16 h, causing a color change from green to light brown with formation of **3** and 1 equiv of $S(SiMe_3)_2$ (1H NMR: δ 0.30; ^{13}C NMR: δ 4.2), as judged by NMR spectroscopy. Volatiles were removed in vacuo, and the resulting solid was washed with pentane (2 mL), extracted into diethyl ether (3 mL), filtered, and dried to afford pure **3** as a yellow-brown solid in quantitative yield (11.0 mg, 99%). 1H NMR (400 MHz, C_6D_6): δ 1.34 (d, 36H + 4H, $-C(CH_3)_3$ +

$P(CH_2)_2P$). $^{13}C\{^1H\}$ NMR (101 MHz, C_6D_6): δ 23.9 (td, J_1 = 17 Hz, J_2 = 4 Hz), CH_2P), 31.1 (s, $C(CH_3)_3$), 36.1 (t, J = 7 Hz, $C(CH_3)_3$), 175.9 (s, $Rh_2(\mu-CS_3)$). $^{31}P\{^1H\}$ NMR (162 MHz, C_6D_6): δ 105.9 (d, $^1J_{RhP}$ = 189 Hz). Anal. Calcd for $C_{37}H_{80}P_4Rh_2S_3$: C, 46.73; H, 8.48. Found: C, 47.05; H, 8.39%.

$(dtbpe)Rh(SC(OSiMe_3))_2N$ (4). Complex **1** (34.2 mg, 0.0588 mmol) was dissolved in C_6D_6 (1.5 mL), split evenly between two Wilmad LPV NMR tubes. Each sample was subjected to two freeze–pump–thaw cycles, warmed to ambient temperature, and had carbonyl sulfide (1 atm) added to it. As the gas entered the solution, the samples immediately changed color from dark green to bright red, and ^{31}P NMR indicated complete conversion (ca. 90% purity) after 10 min. Solvents were removed in vacuo to afford a red solid that was dissolved in minimal pentane (ca. 1 mL) and crystallized by cross diffusion with HMDSO at −35 °C, giving a small crop of **4** as bright red prisms (15.0 mg, 36%). Crystals of **4** recovered in this manner were unstable, losing crystallinity upon warming, which limited the quality of crystallographic data that could be obtained. Although these crystals afford suitable microanalysis data, there is a small impurity (ca. 2%) present in crystalline **4** evident by ^{31}P and 1H NMR, which is likely an unsymmetrical isomer of **4** based on its inequivalent phosphine and trimethylsilyl environments. 1H NMR (400 MHz, C_6D_6): δ 0.40 (s, 18H, $OSi(CH_3)_3$), 1.29 (d, $^3J_{PH}$ = 11.8 Hz, 36H, $-C(CH_3)_3$), 1.38 (d, $^2J_{PH}$ = 11.7 Hz, 4H, $P(CH_2)_2P$). $^{13}C\{^1H\}$ NMR (101 MHz, C_6D_6): δ 1.0 ($OSi(CH_3)_3$), 24.1 (t, J = 18 Hz, CH_2P), 31.0 (s, $C(CH_3)_3$), 36.7 (t, J = 7 Hz, $C(CH_3)_3$), 184.3 ($SC(OSiMe)_3N$). $^{31}P\{^1H\}$ NMR (162 MHz, C_6D_6): δ 91.6 (d, $^1J_{RhP}$ = 160 Hz). Minor impurity (ca. 2%): 1H NMR (C_6D_6): 0.12 (s, 9H), 0.38 (s, 9H), 1.06 (d, J = 12.9 Hz, 18H), 1.16 (d, J = 12.7 Hz, 18H). ^{31}P NMR (162 MHz, C_6D_6): δ 84.6 (dd, $^1J_{PP}$ = 127 Hz, $^2J_{PP}$ = 21 Hz), 105.5 (dd, $^1J_{RhP}$ = 139 Hz, $^2J_{PP}$ = 21 Hz), 84.6 (dd, $^1J_{PP}$ = 127 Hz, $^2J_{PP}$ = 21 Hz). Anal. Calcd for $C_{26}H_{58}NO_2P_2RhS_2Si_2$: C, 44.49; H, 8.33; N, 2.00. Found: C, 44.61; H, 8.18; N, 2.19%.

$[(dtbpe)Rh]_2(\mu-PhNCN)_2$ (5). To a solution of complex **1** (16.3 mg, 0.0280 mmol) in benzene (2 mL) was added phenyl isocyanate (3.5 mg, 0.029 mmol, 1.0 equiv) as a solution in benzene (400 μL). The reaction was allowed to proceed for 24 h, and NMR analysis showed a 1:1 mixture of **1** and **5**. Additional phenyl isocyanate (3.5 mg, 0.029 mmol, 1.0 equiv) was added as a solution in benzene (400 μL), and the reaction was allowed to proceed for 24 h at ambient temperature and 48 h at 70 °C in a sealed vial to ensure maximum conversion to **5**. Volatiles were removed in vacuo, and the residues were extracted into pentane (2 mL) and filtered; crystalline **5** (5.6 mg, 37%) was obtained by slow evaporation of solvent at ambient temperature. Crystals utilized for X-ray diffraction studies were obtained from a concentrated solution of **5** in diethyl ether by cross diffusion with HMDSO at −35 °C. 1H NMR (400 MHz, C_6D_6): δ 1.16 (d, J = 11.2 Hz, 4H, $P(CH_2)_2P$), 1.27 (d, J = 11.1 Hz, 18H + 4H, $-C(CH_3)_3$ + $P(CH_2)_2P$), 1.39 (d, J = 11.4 Hz, 18H, $-C(CH_3)_3$), 1.46 (d, J = 11.3 Hz, 18H, $-C(CH_3)_3$), 1.53 (d, J = 11.1 Hz, 18H, $-C(CH_3)_3$), 6.69 (tt, J_1 = 7.3 Hz, J_2 = 1.1 Hz, 2H, $Ar-H_{para}$), 7.10–7.15 (m, 4H, $Ar-H$), 7.62–7.67 (m, 4H, $Ar-H$). $^{13}C\{^1H\}$ NMR (101 MHz, C_6D_6): δ 23.2–24.4 (m, CH_2P), 30.8 ($C(CH_3)_3$), 31.0 ($C(CH_3)_3$), 31.4 ($C(CH_3)_3$), 31.6 ($C(CH_3)_3$), 35.6 (t, J = 7 Hz, $C(CH_3)_3$), 36.0–36.3 (m, $C(CH_3)_3$), 36.4–36.7 (m, $C(CH_3)_3$), 119.4, 122.2, 131.1, 150.8. $^{31}P\{^1H\}$ NMR (162 MHz, C_6D_6): δ 100.7 (d, $^1J_{RhP}$ = 195 Hz), 112.5 (d, $^1J_{RhP}$ = 194 Hz). IR (CH_2Cl_2 , NaCl, cm^{-1}): 2157 (ν_{NCN}). Anal. Calcd for $C_{50}H_{96}N_4P_4Rh_2$: C, 55.76; H, 8.42; N, 5.20. Found: C, 55.27; H, 8.63; N, 4.78%.

$(dtbpe)Rh(CO)(CN)$ (6). Complex **1** (22.1 mg, 0.0380 mmol) was dissolved in C_6D_6 (600 μL) and added to a Wilmad LPV NMR tube, subjected to two freeze–pump–thaw cycles, warmed to ambient temperature, and carbon monoxide (1 atm) added. Over a period of ca. 5 min, the color of the solution changed from dark green to yellow-brown. After 15 min, analysis by NMR spectroscopy showed a mixture of the desired product **6** and intermediate **1-CO** (80:20). The reaction was allowed to proceed for 16 h, after which yellow crystals of **6** had formed in the NMR tube. Additional CO (1 atm) was added, facilitating completion of the reaction in less than 5 min. The

crystalline material (9.4 mg) was set aside for microanalysis, and additional product was obtained as a yellow film (4.2 mg) by removing volatile components from the supernatant (overall yield: 13.6 mg, 75%). ^1H NMR (400 MHz, C_6D_6): δ 0.95 (d, $^3J_{\text{PH}} = 13.1$ Hz, 18H, $-\text{C}(\text{CH}_3)_3$), 1.24 (d, $^3J_{\text{PH}} = 12.9$ Hz, 18H, $-\text{C}(\text{CH}_3)_3$), 1.2–1.35 (m, 4H, $\text{P}(\text{CH}_2)_2\text{P}$). $^{13}\text{C}\{^1\text{H}\}$ NMR (101 MHz, C_6D_6): δ 23.3 (t, $J = 17$ Hz, CH_2P), 24.1 (t, $J = 16$ Hz, CH_2P), 30.1 (d, $^2J_{\text{PC}} = 5$ Hz, $\text{C}(\text{CH}_3)_3$), 30.6 (d, $^2J_{\text{PC}} = 5$ Hz, $\text{C}(\text{CH}_3)_3$), 35.9–36.3 (m, $\text{C}(\text{CH}_3)_3$) [Note: CO and CN ligands were not observed by ^{13}C NMR spectroscopy when unlabeled CO was used for the reaction]. $^{31}\text{P}\{^1\text{H}\}$ NMR (162 MHz, C_6D_6): δ 93.0 (dd, $^1J_{\text{RHP}} = 125$ Hz, $^2J_{\text{PP}} = 20$ Hz), 106.5 (dd, $^1J_{\text{RHP}} = 122$ Hz, $^2J_{\text{PP}} = 20$ Hz). IR (CH_2Cl_2 , NaCl, cm^{-1}): 2104 (ν_{CN}), 1998 (ν_{CO}). Anal. Calcd for $\text{C}_{20}\text{H}_{40}\text{NOP}_2\text{Rh}$: C, 50.53; H, 8.48; N, 2.95. Found: C, 51.00; H, 8.42; N, 3.01%.

(dtbpe)Rh(^{13}CO)(^{13}CN) ($6(^{13}\text{C})$). Complex **1** (ca. 12 mg) was dissolved in C_6D_6 (700 μL) and added to a Wilmad LPV NMR tube, subjected to three freeze–pump–thaw cycles, warmed to ambient temperature, and had carbon- ^{13}C monoxide (0.5 atm) added to it, causing an immediate color change from dark green to golden. After 1 h, NMR analysis showed a mixture of **6**(^{13}C) and **1**- ^{13}CO . The sample was subjected to one freeze–pump–thaw cycle, and carbon- ^{13}C monoxide (1 atm) was added, leading to immediate completion of the reaction, as judged by ^{31}P NMR spectroscopy. The product was obtained in pure form as a yellow powder by lyophilization from benzene. Key spectral data: $^{13}\text{C}\{^1\text{H}\}$ NMR (101 MHz, C_6D_6): δ 134.3–136.6 (br m, Rh–CN), 190.7 (dddd, $^2J_{\text{PC}(\text{trans})} = 100$ Hz, $^1J_{\text{RhC}} = 64$ Hz, $^2J_{\text{PC}(\text{cis})} = 13$ Hz, $^2J_{\text{CC}} = 7$ Hz). ^{31}P NMR (162 MHz, C_6D_6): δ 93.0 (dddd, $^1J_{\text{RHP}} = 121$ Hz, $^2J_{\text{PC}(\text{trans})} = 100$ Hz, $^2J_{\text{PP}} = 20$ Hz, $^2J_{\text{PC}(\text{cis})} = 19$ Hz), 106.5 (dddd, $^1J_{\text{RHP}} = 123$ Hz, $^2J_{\text{PC}(\text{trans})} = 83$ Hz, $^2J_{\text{PP}} = 20$ Hz, $^2J_{\text{PC}(\text{cis})} = 13$ Hz). IR (CH_2Cl_2 , NaCl, cm^{-1}): 2059 ($\nu_{13\text{CN}}$), 1952 ($\nu_{13\text{CO}}$).

X-ray Crystallography. Single-crystal X-ray diffraction data for compounds **2** and **4** were collected on a Rigaku XtaLAB mini diffractometer using Mo $K\alpha$ radiation ($\lambda = 0.71073$ Å). The diffractometer was equipped with an Oxford Cryosystems desktop cooler (Oxford Cryosystems Ltd., Oxford) for low-temperature data collection. The crystals were mounted on a MiTeGen micromount (MiTeGen, LLC, Ithaca, NY) using STP oil. The frames were integrated using CrystalClear-SM Expert 3.1 b27³¹ to give the *hkl* files corrected for Lorentz polarization and decay. Data were corrected for absorption effects using a multiscan method (REQAB).³¹

Single-crystal X-ray diffraction data for compounds **3** and **5** were collected at the University of Minnesota X-ray crystallographic laboratory on a Bruker APEX II Platform CCD diffractometer using Mo $K\alpha$ radiation ($\lambda = 0.71073$ Å, **3**) or Cu $K\alpha$ radiation ($\lambda = 1.54178$ Å, compound **5**). The data intensities were corrected for absorption and decay (SADABS). Final cell constants were obtained from least-squares fits of all measured reflection.

All structures were solved using SHELXS-2013 and refined using SHELXL-2013 with the Olex2 software package.³² All non-hydrogen atoms were refined with anisotropic thermal parameters. ORTEP drawings were prepared using ORTEP-3 for Windows V2013.1³³ and POV-Ray for Windows v3.6.³⁴ Tabulated crystallographic parameters are presented in Supporting Information, Table S1.

■ ASSOCIATED CONTENT

■ Supporting Information

NMR spectra for all reported complexes, tabulated X-ray crystallographic data, and crystallographic data in CIF format for complexes **2**–**5**. This material is available free of charge via the Internet at <http://pubs.acs.org>. Additionally, crystallographic data for the complexes have been deposited at the Cambridge Crystallographic Data Centre (Nos. 1047433–1047446) and can be obtained free of charge via www.ccdc.cam.ac.uk.

■ AUTHOR INFORMATION

Corresponding Author

*E-mail: mwhited@carleton.edu.

Notes

The authors declare no competing financial interest.

■ ACKNOWLEDGMENTS

The authors acknowledge funding through a Cottrell College Science Award from the Research Corporation for Science Advancement. X-ray crystallography was supported by NSF-MRI Award No. 1125975, “MRI Consortium: Acquisition of a Single Crystal X-ray Diffractometer for a Regional PUI Molecular Structure Facility”, and NMR spectroscopy was enabled by NSF-MRI Award No. 1428752, “MRI: Acquisition of a 400 MHz NMR Spectrometer to Support Research and Undergraduate Research Training at Carleton College and St. Olaf College”. V. Young (UMN) provided crystallographic assistance for complexes **3** and **5**. Additional support was provided by startup funds from Carleton College.

■ REFERENCES

- (1) For leading references, see: Hartwig, J. F. *Organotransition Metal Chemistry: From Bonding to Catalysis*; University Science Books: Sausalito, CA, 2010.
- (2) (a) Lappert, M. F.; Power, P. P.; Sanger, A. R.; Srivastava, R. C. *Metal and Metalloid Amides*; Ellis Horwood: Chichester, U.K., 1980. (b) Lappert, M. F.; Protchenko, A. V.; Power, P. P.; Seeber, A. L. *Metal Amide Chemistry*; Wiley: West Sussex, 2008. (c) Bryndza, H. E.; Tam, W. *Chem. Rev.* **1988**, *88*, 1163.
- (3) (a) Burger, H.; Wannagat, U. *Monatsh. Chem.* **1963**, *94*, 1007. (b) Power, P. P. *J. Organomet. Chem.* **2004**, *689*, 3904. (c) Power, P. P. *Chem. Rev.* **2012**, *112*, 3482.
- (4) (a) Fryzuk, M. D.; Macneil, P. A. *J. Am. Chem. Soc.* **1981**, *103*, 3592. (b) Fryzuk, M. D. *Can. J. Chem.* **1992**, *70*, 2839. (c) Fryzuk, M. D.; Gao, X. L.; Joshi, K.; Macneil, P. A.; Massey, R. L. *J. Am. Chem. Soc.* **1993**, *115*, 10581. (d) Fryzuk, M. D.; Leznoff, D. B.; Thompson, R. C.; Rettig, S. J. *J. Am. Chem. Soc.* **1998**, *120*, 10126. (e) Watson, L. A.; Ozerov, O. V.; Pink, M.; Caulton, K. G. *J. Am. Chem. Soc.* **2003**, *125*, 8426. (f) Walstrom, A.; Pink, M.; Yang, X. F.; Tomaszewski, J.; Baik, M. H.; Caulton, K. G. *J. Am. Chem. Soc.* **2005**, *127*, 5330. (g) Ingleson, M.; Fan, H. J.; Pink, M.; Tomaszewski, J.; Caulton, K. G. *J. Am. Chem. Soc.* **2006**, *128*, 1804.
- (5) (a) Fryzuk, M. D.; Macneil, P. A. *J. Am. Chem. Soc.* **1984**, *106*, 6993. (b) Freundlich, J. S.; Schrock, R. R.; Davis, W. M. *J. Am. Chem. Soc.* **1996**, *118*, 3643. (c) Ozerov, O. V.; Gerard, H. F.; Watson, L. A.; Huffman, J. C.; Caulton, K. G. *Inorg. Chem.* **2002**, *41*, 5615. (d) Fryzuk, M. D.; Shaver, M. P.; Patrick, B. O. *Inorg. Chim. Acta* **2003**, *350*, 293. (e) Bailey, B. C.; Basuli, F.; Huffman, J. C.; Miodiola, D. J. *Organometallics* **2006**, *25*, 2725. (f) Ishiwata, K.; Kuwata, S.; Ikariya, T. *Dalton Trans.* **2007**, 3606. (g) Fullmer, B. C.; Fan, H.; Pink, M.; Caulton, K. G. *Inorg. Chem.* **2008**, *47*, 1865. (h) Sattler, W.; Parkin, G. *J. Am. Chem. Soc.* **2011**, *133*, 9708. (i) Schau-Magnussen, M.; Malcho, P.; Herbst, K.; Brorson, M.; Bendix, J. *Dalton Trans.* **2011**, *40*, 4212.
- (6) (a) Whited, M. T. *Beilstein J. Org. Chem.* **2012**, *8*, 1554. (b) Whited, M. T.; Kosanovich, A. J.; Janzen, D. E. *Organometallics* **2014**, *33*, 1416. (c) Whited, M. T.; Deetz, A. M.; Boerma, J. W.; DeRossa, D. E.; Janzen, D. E. *Organometallics* **2014**, *33*, 5070.
- (7) (a) Bianchini, C.; Ghilardi, C. A.; Meli, A.; Midollini, S.; Orlandini, A. *Inorg. Chem.* **1985**, *24*, 932. (b) Shaver, A.; Lum, B. S.; Bird, P.; Arnold, K. *Inorg. Chem.* **1989**, *28*, 1900. (c) Shaver, A.; Plouffe, P. Y.; Bird, P.; Livingstone, E. *Inorg. Chem.* **1990**, *29*, 1826. (d) Shaver, A.; El-khateeb, M.; Lebus, A. M. *Inorg. Chem.* **2001**, *40*, 5288. (e) Arroyo, M.; Bernes, S.; Ceron, J.; Rius, J.; Torrens, H. *Inorg. Chem.* **2004**, *43*, 986. (f) Chen, Y. H.; Peng, Y.; Chen, P. P.; Zhao, J.

- F.; Liu, L. T.; Li, Y.; Chen, S. Y.; Qu, J. P. *Dalton Trans.* **2010**, 39, 3020.
- (8) McKenna, M.; Wright, L. L.; Miller, D. J.; Tanner, L.; Haltiwanger, R. C.; Dubois, M. R. *J. Am. Chem. Soc.* **1983**, 105, 5329.
- (9) (a) Bianchini, C.; Innocenti, P.; Meli, A. *J. Chem. Soc., Dalton Trans.* **1983**, 1777. (b) Fornies, J.; Uson, M. A.; Gil, J. I.; Jones, P. G. *J. Organomet. Chem.* **1986**, 311, 243.
- (10) (a) Li, B.; Tan, X.; Xu, S. S.; Song, H. B.; Wang, B. Q. *J. Organomet. Chem.* **2008**, 693, 667. (b) Lam, O. P.; Castro, L.; Kosog, B.; Heinemann, F. W.; Maron, L.; Meyer, K. *Inorg. Chem.* **2012**, 51, 781.
- (11) Oster, S. S.; Jones, W. D. *Inorg. Chim. Acta* **2004**, 357, 1836.
- (12) Wright, L. L.; Haltiwanger, R. C.; Noordik, J.; Dubois, M. R. *J. Am. Chem. Soc.* **1987**, 109, 282.
- (13) (a) Axtell, A. T.; Cobley, C. J.; Klosin, J.; Whiteker, G. T.; Zanotti-Gerosa, A.; Abboud, K. A. *Angew. Chem., Int. Ed.* **2005**, 44, 5834. (b) Axtell, A. T.; Klosin, J.; Abboud, K. A. *Organometallics* **2006**, 25, 5003. (c) Thibault, M. H.; Tay, M. G.; Batsanov, A. S.; Howard, J. A. K.; Marder, T. B. *J. Organomet. Chem.* **2013**, 730, 104.
- (14) (a) Ebsworth, E. A. V.; Rocktäschel, G.; Thompson, J. C. *J. Chem. Soc. A* **1967**, 362. (b) Yoder, C. H.; Komoriya, A.; Kochanowski, J. E.; Suydam, F. H. *J. Am. Chem. Soc.* **1971**, 93, 6515.
- (15) The unit cell of the colorless crystals obtained from CH₂Cl₂/pentane matched that of CCDC #286373: $a = 18.26 \text{ \AA}$, $b = 16.08 \text{ \AA}$, $c = 8.32 \text{ \AA}$, $\alpha = 90^\circ$, $\beta = 98.9^\circ$, $\gamma = 90^\circ$.
- (16) Wang, H. M.; Li, H. X.; Yu, X. Y.; Ren, Z. G.; Lang, J. P. *Tetrahedron* **2011**, 67, 1530.
- (17) (a) Ainscough, E. W.; Brodie, A. M.; Healy, P. C.; Waters, J. M. *Aust. J. Chem.* **2000**, 53, 971. (b) Crutchley, R. J. *Coord. Chem. Rev.* **2001**, 219, 125. (c) Escuer, A.; Mautner, F. A.; Sanz, N.; Vicente, R. *Polyhedron* **2004**, 23, 1409.
- (18) Tanabe, Y.; Kuwata, S.; Ishii, Y. *J. Am. Chem. Soc.* **2002**, 124, 6528.
- (19) The infrared absorbance for the NCN stretch also has a shoulder, suggesting that it represents energetically similar and partially overlapping symmetric and antisymmetric stretching modes.
- (20) (a) Castro-Rodriguez, I.; Nakai, H.; Meyer, K. *Angew. Chem., Int. Ed.* **2006**, 45, 2389. (b) Tran, B. L.; Pink, M.; Gao, X. F.; Park, H.; Mindiola, D. J. *J. Am. Chem. Soc.* **2010**, 132, 1458.
- (21) Babcock, J. R.; Sita, L. R. *J. Am. Chem. Soc.* **1998**, 120, 5585.
- (22) Zarusnitskii, E. V.; Pervak, I. I.; Merkulov, A. S.; Yurchenko, A. A.; Tolmachev, A. A.; Pinchuk, A. M. *Synthesis* **2006**, 1279.
- (23) (a) Wu, Y. J.; Wang, S. W.; Zhu, X. C.; Yang, G. S.; Wei, Y.; Zhang, L. J.; Song, H. B. *Inorg. Chem.* **2008**, 47, 5503. (b) Zhu, X. C.; Fan, J. X.; Wu, Y. J.; Wang, S. W.; Zhang, L. J.; Yang, G. S.; Wei, Y.; Yin, C. W.; Zhu, H.; Wu, S. H.; Zhang, H. T. *Organometallics* **2009**, 28, 3882.
- (24) (a) *CRC Handbook of Chemistry and Physics*, 77th ed.; Lide, D. R., Ed.; CRC Press: Boca Raton, FL, 1996. (b) Zumdahl, S. S.; Zumdahl, S. A. *Chemistry*, 9th ed.; Brooks Cole: Belmont, CA, 2014.
- (25) Johnson, C. E.; Fisher, B. J.; Eisenberg, R. *J. Am. Chem. Soc.* **1983**, 105, 7772.
- (26) Sellmann, D.; Geipel, F.; Heinemann, F. W. *Chem.—Eur. J.* **2000**, 6, 4279.
- (27) Sattler, W.; Parkin, G. *Chem. Commun.* **2009**, 7566.
- (28) Wannagat, U.; Seyffert, H. *Angew. Chem., Int. Ed.* **1965**, 4, 438.
- (29) Semproni, S. P.; Chirik, P. J. *J. Am. Chem. Soc.* **2013**, 135, 11373.
- (30) Werner, H.; Bosch, M.; Schneider, M. E.; Hahn, C.; Kukla, F.; Manger, M.; Windmuller, B.; Weberndorfer, B.; Laubender, M. *J. Chem. Soc., Dalton Trans.* **1998**, 3549.
- (31) *CrystalClear*; Rigaku Americas and Rigaku: The Woodlands, TX, 2011.
- (32) Dolomanov, O. V.; Bourhis, L. J.; Gildea, R. J.; Howard, J. A. K.; Puschmann, H. *J. Appl. Crystallogr.* **2009**, 42, 339.
- (33) Farrugia, L. J. *J. Appl. Crystallogr.* **2012**, 45, 849.
- (34) *Persistence of Vision Raytracer (Version 3.6)*; Persistence of Vision Pty. Ltd.: Williamstown, Victoria, Australia, 2004.
- (35) Nelsen, E. R.; Landis, C. R. *J. Am. Chem. Soc.* **2013**, 135, 9636.